Several experimental realizations of symmetric phase-covariant quantum cloners of single-photon qubits

Jan Soubusta,[1] Lucie Bartůšková,[2] Antonín Černoch,[1] Jaromír Fiurášek,[2] and Miloslav Dušek[2]

[1]*Joint Laboratory of Optics of Palacký University and Institute of Physics of Academy of Sciences of the Czech Republic,
17. listopadu 50A, 779 07 Olomouc, Czech Republic*

[2]*Department of Optics, Palacký University, 17. listopadu 50, 772 00 Olomouc, Czech Republic*

We compare several optical implementations of phase-covariant cloning machines. The experiments are based on copying of the polarization state of a single photon in bulk optics by a special unbalanced beam splitter or by a balanced beam splitter accompanied by a state filtering. Also the all-fiber-based setup is discussed, where the information is encoded into spatial modes, i.e., the photon can propagate through two optical fibers. Each of the four implementations possesses some advantages and disadvantages that are discussed.

I. INTRODUCTION

One of the most fundamental consequences of the laws of quantum mechanics is the impossibility of an exact copying of an unknown quantum state [1]. Nevertheless, this no-go statement does not exclude a possibility of an approximate copying [2]. In general, quantum cloning machines can create M approximate clones from $N < M$ originals. The simplest ones produce two approximate copies from one original unknown qubit state using one ancilla qubit. The quality of cloning can be well quantified by the measure of fidelity, which is defined as the overlap of each copy with the original input state. Optimal cloners maximize average fidelities of the clones. In the symmetric case the fidelities of all clones are equal. Asymmetric cloning transformations allow different fidelities of particular clones, i.e., smaller distortion of some copies at the cost of lower precision of the others. The theory of optimal quantum cloners is well established and optimal cloning transformations are known for many classes of input states [3,4].

In optical realizations of quantum information processing, one is mostly interested in cloning of the states of single photons. Most experimental realizations up to now implemented a universal cloning transformation using either stimulated parametric down conversion [5–7] or interference of photons on a balanced beam splitter [8–10]. In the case of a universal cloner, fidelities of the clones do not depend on the input state to be copied [2,11]. Sometimes, however, we want to clone only a certain subset of states and in this case a higher fidelity may be obtained using an appropriately tailored cloner. In particular, the *phase-covariant* cloning machine optimally clones all qubit states from the equator of the Bloch sphere [12–15]. More precisely, fidelities of cloned qubit states produced by a phase-covariant cloning transformation do not depend on the mutual phase between amplitudes of two fixed-basis states $|0\rangle$ and $|1\rangle$ but depend on their "intensity" ratio. For a subset of states with a fixed intensity ratio the optimal phase-covariant cloner offers higher fidelities of clones than the universal one. Phase-covariant cloner is of great interest also because it can be used for an optimal individual attack on BB84 quantum key distribution protocol

[3]. Besides eavesdropping, quantum cloning can be also used to perform minimal disturbance measurement of a single qubit or to enhance the transmission fidelity over a lossy quantum channel [16].

In this paper we describe several different experimental realizations of the optimal symmetric phase-covariant $1 \rightarrow 2$ cloning of optical qubit states and compare their performances. The schemes that we consider can be broadly divided into two categories. The first approach to cloning of polarization states of single photons relies on the two-photon interference on a specially tailored unbalanced beam splitter, which exhibits different transmittance for vertical and horizontal polarizations [17]. Besides the scheme utilizing a special custom-made beam splitter that was described in our earlier publication [18], we also present and investigate a setup where the unbalanced beam splitter is emulated by a Mach-Zehnder interferometer [19] with a Soleil-Babinet compensator in each arm.

We also propose and demonstrate a second alternative approach to optimal phase-covariant cloning, which combines the bunching of photons on a balanced beam splitter followed by a state-dependent filtering operation. With this latter method we were able to demonstrate high-quality phase-covariant cloning of polarization states of single photons, with average fidelities exceeding the limit of optimal universal cloning.

For completeness, we also briefly review the all-fiber-based cloning scheme, where the qubits are encoded in a state of a single photon, which can propagate in two different single-mode optical fibers [20]. This scheme represents again the first cloning approach, where two variable ratio couplers stand in for the special beam splitter. With this last setup we were able to accomplish high-quality phase-covariant cloning of single-photon states encoded into spatial modes. The average fidelities exceed the limit of optimal universal cloning.

The article is organized as follows. Section II recapitulates briefly the basic theoretical tools and describes theoretically the different possible implementations of a phase-covariant cloning machine. Section III deals with an implementation employing a Mach-Zehnder interferometer
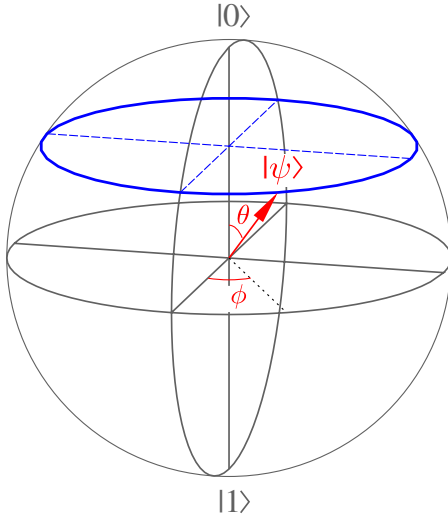
FIG. 1. (Color online) States with the same latitude on the Bloch sphere, i.e., states with fixed "intensity" ratio of basis states $|0\rangle$ and $|1\rangle$. θ and ϕ represent the spherical coordinates of latitude and longitude, respectively.

in the role of a beam splitter with different splitting ratios for different polarization components. In Sec. IV the system is reported which uses a custom-made beam splitter with similar properties. The phase-covariant cloner based on state filtration that combines fiber and bulk optics is described in Sec. V. Implementation fully based on fiber optics and spatial-mode encoding is addressed in Sec. VI. Finally, Sec. VII summarizes the results and compares different experimental platforms.

II. THEORY

In this paper we are interested in optimal copying of single-qubit states $|\psi\rangle$, which form a two-dimensional Hilbert space spanned by computational basis states $|0\rangle$ and $|1\rangle$ and can be parametrized by two angles θ and ϕ,

$$|\psi\rangle = \cos\frac{\theta}{2}|0\rangle + e^{i\phi}\sin\frac{\theta}{2}|1\rangle. \tag{1}$$

These states can be visualized as points on the surface of the Bloch sphere (see Fig. 1). Note that θ and ϕ represent the spherical coordinates of these points, i.e., the latitude and longitude, respectively. In certain applications such as eavesdropping on quantum key distribution protocols, one only needs to copy states that have a fixed latitude θ on the Bloch sphere. In this case the best strategy is to employ an appropriate *phase-covariant* cloner that optimally exploits this *a priori* information and provides higher fidelities of the clones than the universal cloner.

The optimal symmetric phase-covariant cloning transformation for the states on the northern hemisphere of the Bloch sphere reads [17,21–23]
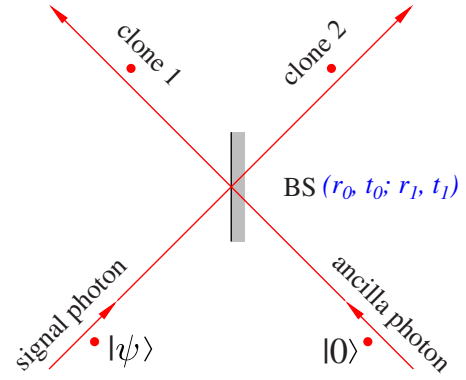
$$|0\rangle \rightarrow |00\rangle,$$

FIG. 2. (Color online) Phase-covariant cloner based on two-photon interference on a special beam splitter with splitting ratio $21:79$ for the basis state $|0\rangle$ and opposite splitting ratio $79:21$ for the other basis state $|1\rangle$.

$$|1\rangle \rightarrow \frac{1}{\sqrt{2}}(|10\rangle + |01\rangle). \tag{2}$$

This transformation produces two approximate clones with identical fidelities. For the states from the southern hemisphere the optimal phase-covariant cloning operation can be obtained simply interchanging the states $|0\rangle$ and $|1\rangle$ in Eq. (2). For the states with the same latitude on the sphere the cloning fidelities are constant. The minimum value of fidelity is obtained for the states from the equator of the Bloch sphere and the fidelities increase up to unity as the signal state approaches the pole [17].

In this paper we focus on the cloning of the equatorial states

$$|\psi\rangle = \frac{1}{\sqrt{2}}(|0\rangle + e^{i\phi}|1\rangle). \tag{3}$$

For this class of states the cloning fidelity reaches the value $F_{\text{ph. cov.}} = \frac{1}{2}(1 + \frac{1}{\sqrt{2}}) \approx 85.4\%$. In comparison the fidelity of the optimal symmetric universal cloning is only $F_{\text{univ}} = \frac{5}{6} \approx 83.3\%$ and the semiclassical limit is $F_{\text{sc}} = 75\%$. By the semiclassical limit we mean the optimal estimation from a single copy of an unknown state from the equator of the Bloch sphere [24] followed by preparation of two copies according to the measurement result.

In most of the experimental schemes presented below we utilize encoding of qubits into polarization degree of freedom of single photons. The basis states $|0\rangle$ and $|1\rangle$ then correspond to two orthogonal polarization states of a single photon, such as vertical, $|V\rangle$, and horizontal, $|H\rangle$, linear polarizations. The transformation (2) can be directly, albeit probabilistically, realized by letting the cloned photon interfere with a second auxiliary photon on a special beam splitter with splitting ratios different for state $|0\rangle$, and for state $|1\rangle$ (or $|V\rangle$ and $|H\rangle$) (see Fig. 2). The cloning succeeds when a single photon appears at each output port of the beam splitter. The resulting conditional transformation can be expressed as

$$|0\rangle_{\text{sig}}|0\rangle_{\text{anc}} \rightarrow (r_0^2 - t_0^2)|00\rangle,$$
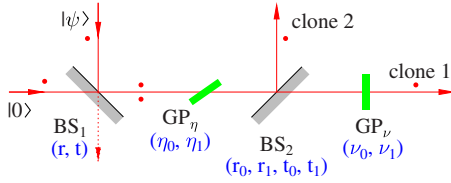
FIG. 3. (Color online) Phase-covariant cloner based on the Hong-Ou-Mandel interference [25] on a balanced beam splitter followed by state filtering.

$$|1\rangle_{\text{sig}}|0\rangle_{\text{anc}} \rightarrow r_0 r_1 |10\rangle - t_0 t_1 |01\rangle, \qquad (4)$$

where r_0, r_1; t_0, t_1 are the amplitude reflectances and transmittances for state $|0\rangle$ and $|1\rangle$, respectively. We have to find conditions under which the action of the beam splitter (4) corresponds to the demanded transformation (2). We immediately find that the following relations must be fulfilled: $r_0 r_1 = -t_0 t_1$ and $(r_0^2 - t_0^2) = \sqrt{2} r_0 r_1$. Assuming an ideal lossless beam splitter satisfying $|r|^2 + |t|^2 = 1$ we obtain the value of the intensity reflectances $R_0 \equiv r_0^2 = \frac{1}{2}(1 + \frac{1}{\sqrt{3}}) \approx 78.9\%$ and $R_1 = 1 - R_0 \approx 21.1\%$. The multiplicative factors in Eq. (4) are related to the probability of success of the scheme $P_{\text{succ 1}} = (r_0^2 - t_0^2)^2 = (2R_0 - 1)^2$, which in the ideal case is equal to $P_{\text{succ 1}} = \frac{1}{3} \approx 33.3\%$ [17].

Another possibility of how to obtain the transformation (2) for polarization states of photons is to start from the implementation of the universal cloner based on photon bunching on a balanced beam splitter [8–10] and modify it by the state filtering (see Fig. 3). The first beam splitter, BS_1, implements a universal cloning. This operation succeeds if both photons leave BS_1 through the same output port. To achieve the optimal phase-covariant copying operation the state filtering is applied to the pair of qubits by means of a tilted glass plate GP_η that introduces polarization-dependent losses. Finally, the two photons are separated at the second beam splitter, BS_2. The full operation is successful if one photon appears at output 1 and simultaneously the other photon at output 2. Slight polarization dependence of the transmittance of BS_2 is compensated by another tilted glass plate GP_ν. The resulting conditional transformation reads

$$|0\rangle_{\text{sig}}|0\rangle_{\text{anc}} \rightarrow 2rt \eta_0^2 t_0 \nu_0 r_0 |00\rangle,$$

$$|1\rangle_{\text{sig}}|0\rangle_{\text{anc}} \rightarrow rt \eta_0 \eta_1 (t_1 \nu_1 r_0 |10\rangle + t_0 \nu_0 r_1 |01\rangle), \qquad (5)$$

where r, t are the coefficients of amplitude reflectances and transmittances of BS_1; r_0, r_1, t_0, t_1 are the coefficients corresponding to BS_2 which, in reality, slightly differ for state $|0\rangle$ and $|1\rangle$; η_0, η_1 and ν_0, ν_1 are amplitude transmittances of the tilted glass plates GP_η and GP_ν, respectively. Again we have to find conditions under which the transformations (5) become equivalent to (2). In this case, the free parameters are the transmittances of the tilted glass plates. The conditions for the symmetric operation read $\nu_0 / \nu_1 = t_1 r_0 / t_0 r_1$ and $\eta_1 / \eta_0 = \sqrt{2} r_0 / r_1$, which determines the tilts of the glass plates. The probability of success $P_{\text{succ 2}} = (2rt \eta_0^2 t_0 \nu_0 r_0)^2$. Here the maximum probability of success reached in ideal conditions is only $P_{\text{succ 2}} = \frac{1}{16} = 6.25\%$.
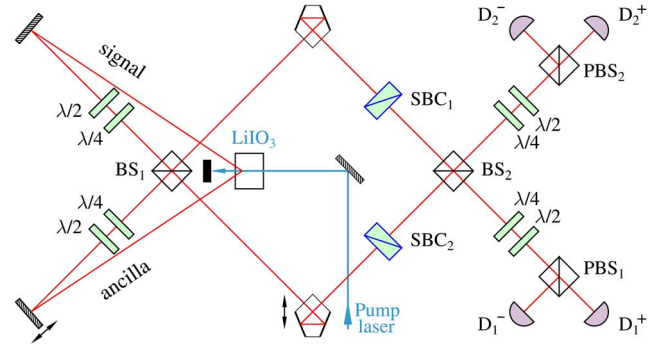

FIG. 4. (Color online) Scheme of the cloning setup based on the Mach-Zehnder interferometer. BS—nonpolarizing cube beam splitter, SBC—Soleil-Babinet compensator, PBS—polarizing cube beam splitter, $\lambda/2, \lambda/4$—wave plates, D—detector.

III. FREE-SPACE REALIZATION WITH THE MACH-ZEHNDER INTERFEROMETER

In bulk optics it is straightforward to use polarization encoding of single-photon qubits. The states $|0\rangle$ and $|1\rangle$ are represented by vertical, V, and horizontal, H, linear polarizations, respectively. One possible way how to simulate a beam splitter with any required splitting ratio is to use an interferometer and stabilize it at a certain point within an interference fringe. The beam splitter with splitting ratios different for vertical and horizontal polarization can be implemented by a Mach-Zehnder (MZ) interferometer with different phase shifts for vertical and horizontal polarization components. Figure 4 shows the experimental setup utilizing the MZ interferometer with a Soleil-Babinet compensator in each arm. With these compensators we can tune the interference fringes separately for V and H polarizations. In this setup one must try to carefully compensate polarization-dependent phase shifts of all used optical components.

Let us assume the case of a perfectly balanced MZ interferometer with two ideal $50:50$ beam splitters without additional phase shifts. The formulas for the reflectances and transmittances for both polarizations reduce to a simple expression.

$$R_j = \sin^2 \vartheta_j, \quad T_j = \cos^2 \vartheta_j, \quad j = V, H, \qquad (6)$$

where ϑ_V, ϑ_H are the phase differences between the MZ interferometer arms for the two respective polarizations.

Figure 4 depicts the whole corresponding experimental cloning setup. The nonlinear crystal of LiIO_3 is pumped by a cw Kr^+ laser at 413 nm. In the crystal, pairs of photons are produced in the process of type I spontaneous parametric down conversion. These photons are tightly correlated in time and horizontally polarized. Arbitrary polarization state $|\psi\rangle$ of the signal photon can be prepared by means of half- and quarter-wave plates ($\lambda/2, \lambda/4$). In a similar way, the ancilla photon is set to a fixed vertically linearly polarized state. Both photons enter the MZ interferometer, which emulates a beam splitter whose splitting ratio is independently tunable for horizontal and vertical polarizations. The MZ interferometer is not perfectly stable. The phase drifts ran-

domly due to temperature changes and air flux. Therefore the whole interferometer is enclosed in a shielding box and besides that, the active stabilization is periodically performed between ten-second measurement steps. The proper phase is set by means of piezocontrolled shifting of a penta prism in one arm of the MZ interferometer (indicated by an arrow in Fig. 4).

The cloning procedure is successful if there is one photon in each output port. The setting of the wave plates at the output ports of the MZ interferometer is inverse with respect to the signal qubit preparation, so a photon with the same polarization as the original signal photon is transmitted through the polarizing beam splitter (PBS) to the detector D^+, whereas the photon with orthogonal polarization is reflected to the detector D^-. Each clone is thus measured in the basis formed by the input state $|\psi\rangle$ and its orthogonal counterpart. In the experiment we measure four coincidence rates C^{ab} of simultaneous clicks of detectors D_1^a and D_2^b, where $a, b = +, -$. For instance, C^{++} denotes the number of simultaneous clicks of detectors D_1^+ and D_2^+, which indicates detection of two perfect clones. The fidelity of the jth clone is then calculated as the fraction of the events when detector D_j^+ fired and the total number of all detection events,

$$F_1 = \frac{C^{++} + C^{+-}}{C_{\text{sum}}},$$

$$F_2 = \frac{C^{++} + C^{-+}}{C_{\text{sum}}}, \tag{7}$$

where $C_{\text{sum}} = C^{++} + C^{+-} + C^{-+} + C^{--}$.

In order to correctly measure C^{ab} we must ensure that the detection efficiencies of all four detectors are identical, otherwise we could obtain biased results. The relative efficiencies can be balanced by several ways. First, we can measure the exact efficiency of each detector and then calculate the fidelity multiplying the measured coincidences accordingly. Second, we can add additional losses in front of each detector (reduce the iris diameter) to balance the efficiencies. Third, we can change the measurement basis and measure all four coincidences in a sequence using only two detectors, therefore it is not necessary to compensate for any differences. We checked that all three methods provide the same results.

Figure 5 shows the measured fidelities of clones of the states from the equator of the Bloch sphere. Despite relatively precise adjustment, the fidelities are below the semiclassical limit. This is caused mainly by the imperfect overlap of spatial modes on the beam splitters, and by the intrinsic phase shifts of the cube nonpolarizing BSs, which are different for reflected and transmitted photons and cannot be fully compensated in our experiment. Partial compensation is possible for some subset of input states, but complete compensation is experimentally unfeasible. Finally, due to the interferometric setup, the phases may slightly drift in the course of measurement.

The probability of success is determined as the ratio of the sum of all coincidence events at the output of the device and the number of photon pairs entering the MZ interferometer.
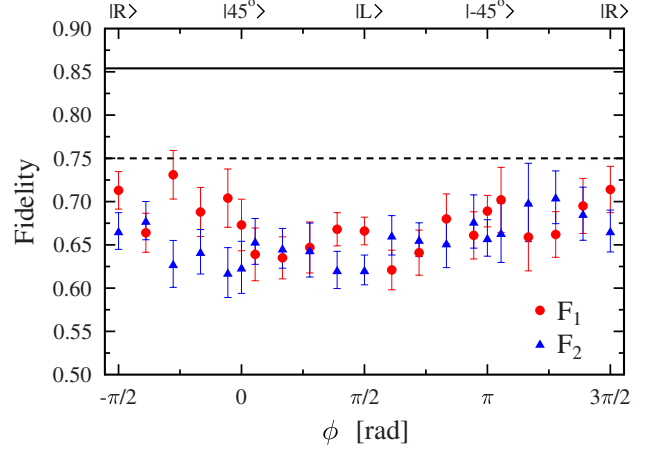

FIG. 5. (Color online) Fidelities of clones measured with the setup based on the MZ interferometer. The full line denotes the theoretical value of fidelity of the phase-covariant cloner. The dashed line shows the semiclassical limit.

The average probability of success, $P_{\text{succ}} = 33.3 \pm 0.2\%$, corresponds well to the theoretical value.

The main advantage of this setup is the possibility to set any splitting ratio, which is essential for asymmetric cloning with tunable asymmetry [20]. The main disadvantages include uncontrollable phase shifts that could not be compensated and nonperfect overlap of the spatial modes on the beam splitters. Consequently, the cloning fidelities were rather low and could not be improved even if we performed spatial-mode filtering by single-mode fibers between the nonlinear crystal and the interferometer.

IV. FREE-SPACE REALIZATION WITH SPECIAL BEAM SPLITTER

If the tunability of the splitting ratio is not desired then an alternative setup with a fixed beam splitter instead of the MZ interferometer is a good choice. We utilized a special beam splitter (manufactured by Ekspla) for this purpose and built a new setup as displayed in Fig. 6. Down-converted photon pairs from the source are coupled into the single-mode fibers, released back into free space and then they enter the cloner. The fibers ensure precise spatial-mode filtering that enhances the overlap of beams on the bulk beam splitter. Because the actual splitting ratios of the BS are not exactly $21:79$ for vertical polarization and $79:21$ for horizontal polarization as required by the theory (given in Sec. II) we compensated them by a tilted glass plate GP. For comparison, we made two series of measurements. The first series was made without any compensation and the measured fidelities of two clones differed by several percent, $F_1 = 84.1 \pm 0.2\%$ and $F_2 = 80.4 \pm 0.2\%$. The probability of success was $P_{\text{succ}} = 31.23 \pm 0.08\%$. The second series of measurements was made introducing polarization-dependent losses in one output by the tilted GP. In this case we achieved more symmetric operation, when the measured fidelities became equal within the measurement error $F_1 = F_2 = 82.2 \pm 0.2\%$
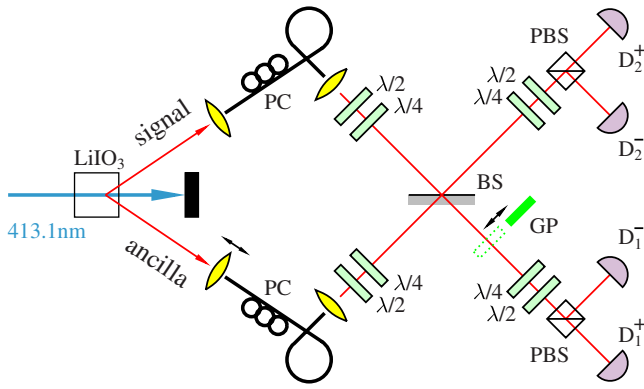
FIG. 6. (Color online) Scheme of the cloning setup based on the specially fabricated beam splitter. BS—special unbalanced plate beam splitter, PBS—polarizing cube beam splitter, PC—polarization controller, GP—compensation glass plate, $\lambda/2$, $\lambda/4$—wave plates, D—detector.

as displayed in Fig. 7. However, these additional losses slightly decreased the probability of success, P_{succ} $=28.8\pm0.1\%$.

The main advantage of this experimental scheme is its simplicity. It essentially generalizes the Hong-Ou-Mandel (HOM) interferometer [25] using a special unbalanced beam splitter. The setup is very stable and compact, losses are minimal, and it is not required to actively stabilize any second-order interference. The spatial-mode filtering by optical fibers increases the overlap of the spatial modes of signal and ancilla photons. Nevertheless, the visibility of HOM-type interference is still not perfect. Using a balanced $50:50$ beam splitter we typically reach values $\approx 92\%$. Consequently, the averaged fidelities of the clones do not exceed the universal cloning limit. The main disadvantage of this setup is that it is possible to tune the asymmetry of the cloner only by applying additional losses, which decreases the prob-
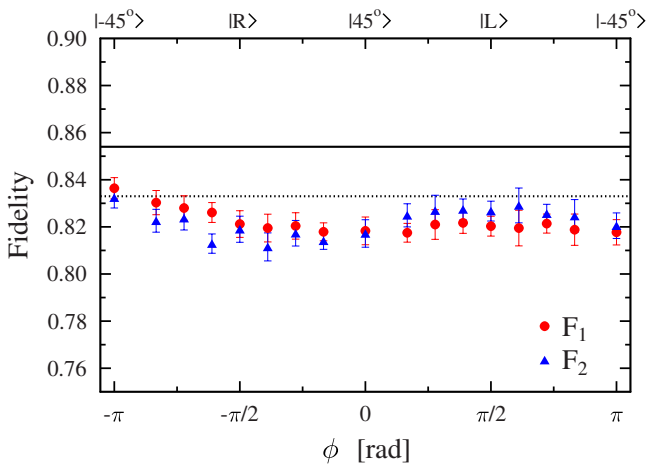

FIG. 7. (Color online) Fidelities of clones measured with the setup based on the special beam splitter together with a compensation glass plate. The full line denotes the theoretical value of fidelity of the phase-covariant cloner. The dotted line shows the limit of the universal cloner.
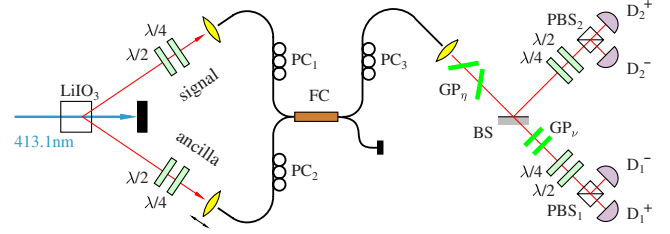

FIG. 8. (Color online) Scheme of the hybrid cloning setup. BS—nonpolarizing beam splitter, PBS—polarizing beam splitter, PC—polarization controller, FC—fiber coupler, $\lambda/2$,$\lambda/4$—wave plates, GP_η,GP_ν—glass plates, D—detector.

ability of success. A more detailed description of this particular setup can be found in Ref. [18].

V. HYBRID SETUP

In order to further increase the cloning fidelities and exceed the fidelity of the optimal universal cloner, $F_{\mathrm{univ}}=\frac{5}{6}$ $\approx 83.3\%$, we have experimentally implemented the cloning scheme based on photon bunching and state filtering depicted in Fig. 3. The resulting hybrid setup combines the advantages of fiber and free-space approaches, and is schematically sketched in Fig. 8. The signal and ancilla photons are coupled into single-mode fibers and interfere in a fiber coupler (FC). Coupling the photon pairs into fibers selects only very well defined spatial modes of the down-converted field. The spatial wave packets of the photons perfectly overlap and the actual splitting ratio of the fiber coupler is $49:51$. These conditions guarantee very high visibility of the HOM interference, typically $\approx 98\%$. The free-space part allows easy handling of the information encoded in the polarization of the photons.

The measurement starts with adjusting the HOM dip. Both fiber outputs from the FC are connected directly to the detectors and the path difference is adjusted in order to maximize the fourth-order interference, i.e., to minimize the coincidence counts. The polarization changes caused by the fibers are compensated using the polarization controllers (PC_1 and PC_2).

Only single output of the FC is used in the cloning operation. In fact, FC implements an optimal universal cloner that is converted to the phase-covariant one by means of state filtering provided by the glass plate GP_η that introduces polarization-dependent losses. After this filtering step, the nonpolarizing beam splitter BS splits the two photons into two different paths with probability $\frac{1}{2}$. The polarization dependence of the splitting ratio of this BS is compensated by polarization-dependent losses introduced by the glass plate GP_ν. Then the polarization analysis is performed in a standard way as in the previous setups. The setting of polarization states of signal and ancilla photons is more complicated here than in the previous cases. First we tilt the PC_3 to adjust the linear vertical polarization of the ancilla photon at the input of BS, while all the wave plates are rotated to zero position. After that the ancilla photon is effectively linearly vertically polarized. The particular signal states are prepared
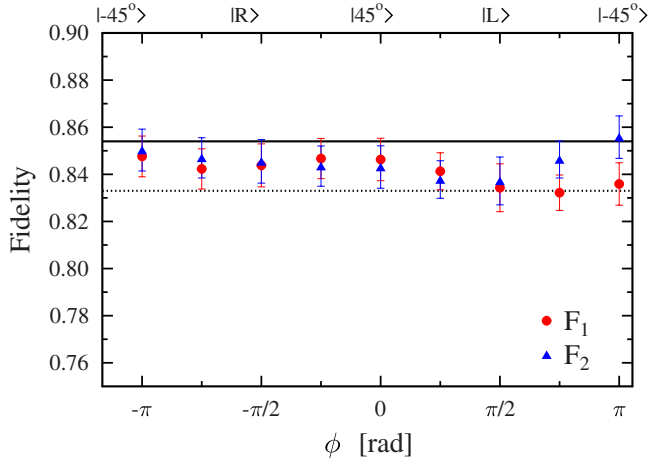
FIG. 9. (Color online) Fidelities of clones measured with the hybrid setup. The full line denotes the theoretical value of fidelity of the phase-covariant cloner. The dotted line shows the limit of the universal cloner.

in a similar way: The ancilla arm is blocked and the measurement polarization bases in the detection blocks are set to select a required polarization state. Then the input polarization is tuned in order to reach the situation when all the signal photons are detected on the detectors D^+ only.

As noted above, without GP_η (without the polarization filtration in front of BS) the setup operates as a well known universal cloning machine [8–10]. Note that the overlap of the vertically polarized ancilla photon with any equatorial state of the signal photon is always $\frac{1}{2}$. For comparison we also measured the fidelities of this universal cloning operation for the same set of input states (not shown here). The mean values of fidelities with this universal cloner were $F_1 = 82.5 \pm 0.9\%$ and $F_2 = 82.5 \pm 0.6\%$, which are very close to the theoretically expected $F_{\text{univ}} \approx 83.3\%$. The fidelities measured with the phase-covariant cloner are shown in Fig. 9. With this device we finally exceeded the universal cloner limit, and achieved mean fidelities $F_1 = 84.1 \pm 0.6\%$ and $F_2 = 84.5 \pm 0.6\%$.

To summarize, the main advantage of the hybrid setup is that it is easy to achieve high visibilities and exceed the universal cloning limit. The disadvantage is the lower probability of success of this cloning scheme; theoretical maximum is $\frac{1}{16} = 6.25\%$. Due to the losses introduced mainly by the compensating glass plates we obtained $P_{\text{succ}} = (4.2 \pm 0.1)\%$. It is also more difficult to properly set the signal and ancilla photon polarization.

VI. FIBER SETUP

The last setup is completely composed of fibers and fiber optics components. The polarization of photon propagating through the fiber undergoes transformations that are hard to trace. Moreover, some fiber components in this setup transmit only one polarization. This makes the encoding of qubits into polarization states in an all-fiber scheme inconvenient. However, our setup utilizes spatial-mode encoding of qubit states (see Fig. 10). Each qubit is represented by a single photon, which can propagate through two different fibers. The presence of the photon in the first (second) fiber corresponds to the basis state $|0\rangle$ ($|1\rangle$). The intensity ratio and phase difference between these two modes determine the state of the qubit, Eq. (1).

Signal and ancilla photons are created by the same source of down-converted photon pairs as mentioned above. The signal photon is split by a fiber coupler FC_0 into fibers f_1, corresponding to the basis state $|1\rangle$, and f_2, corresponding to state $|0\rangle$. With this setup we have experimentally realized the cloning of equatorial qubit states, Eq. (3). Therefore unequal losses in optical fibers f_1 and f_2 are balanced using the attenuator A_0. Various states from the equator are prepared by applying appropriate voltage to the phase modulator PM_0, which sets the relative phase ϕ. The ancilla photon is always in the fixed state $|0\rangle$ corresponding to the single photon propagating exclusively through fiber f_3.

The cloning procedure is accomplished by two variable-ratio couplers $VRC_{|0\rangle}$ and $VRC_{|1\rangle}$, where the first one forms the core of the HOM interferometer. Before starting the final measurement, the splitting ratio of $VRC_{|0\rangle}$ is set to $50:50$ and the HOM dip is adjusted similarly as in the case of the hybrid setup. The visibility of the fourth-order interference is typically $\approx 98\%$. Then the splitting ratio of $VRC_{|0\rangle}$ is changed to the desired value $79:21$, whereas the reverse splitting ratio $21:79$ is set on $VRC_{|1\rangle}$.

Both MZ interferometers are adjusted using only the signal beam from the nonlinear crystal. First the intensities between arms of each MZ interferometer are balanced with the help of attenuators in the detection part of the setup (the part behind VRCs). Visibilities are maximized by precisely balancing the optical lengths in both arms and aligning polarizations in each interferometer. We typically reached visibilities of the second-order interference about 97%. After this we set damping factors in the detection parts such as to ensure projections onto the states on the equator of the Bloch sphere.

Fluctuations of temperature and temperature gradients cause a random phase drift between the arms of each MZ
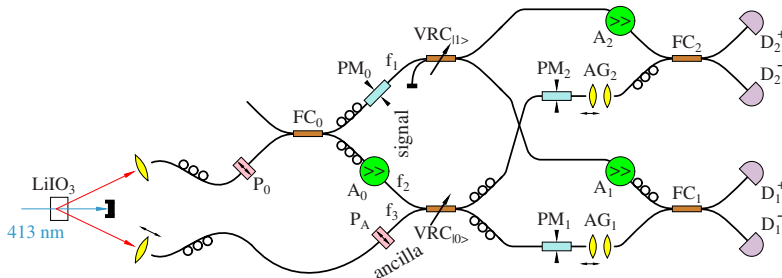

FIG. 10. (Color online) Scheme of the all-fiber cloning setup: P—polarizer, FC—fiber coupler, A—attenuator, PM—phase modulator, VRC—variable ratio coupler, AG—air gap, D—detector.
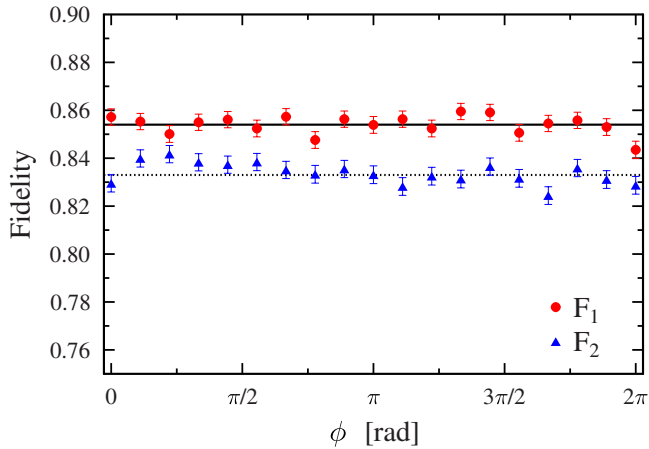
FIG. 11. (Color online) Fidelities of clones measured with the all-fiber setup. The full line denotes the theoretical value of fidelity of the phase-covariant cloner. The dotted line shows the limit of the universal cloner.

TABLE I. Compared values of fidelities F_1, F_2 and total clone rates C_{sum} for all four devices.

Cloner type	F_1	F_2	C_{sum}
Mach-Zehnder	67%	66%	1700/s
Special BS	82.2%	82.2%	3780/s
Hybrid	84.1%	84.5%	680/s
Fiber	85.4%	83.4%	60/s

interferometer. Therefore the experimental setup is thermally isolated in a polystyrene box and additionally an active stabilization is periodically performed between three-second measurement steps. Only signal beam from the crystal is used for the stabilization, the other one is blocked. In each stabilization cycle values of both phase drifts are simultaneously estimated and they are compensated by means of phase modulators in the detection part of the setup.

The cloning operation is successful only if there is one photon detected by each pair of detectors (D^+, D^-). Fidelities of the clones are measured using two detection blocks consisting of the phase modulators, the attenuators, and 50:50 fiber couplers. The projection onto the particular signal state is realized by the setting of proper phase shifts by phase modulators PM_1 and PM_2. Unequal detector efficiencies are compensated by proper rescaling of the measured coincidence rates according to the relative detector efficiencies. We also checked that the same fidelities are obtained from the coincidences measured only by one pair of detectors. Figure 11 shows fidelities calculated from the data acquired by 40 three-second measurement steps for each phase. Note that this long measurement period compensates low coincidence count rate and results in small statistical errors. The cloning fidelities averaged over all measured states are $F_1 = 85.4 \pm 0.4\%$ and $F_2 = 83.4 \pm 0.4\%$. They differ by 2.0%, which is probably the consequence of nonideal splitting ratios, differing from 50:50, of the couplers FC_1 and FC_2 in the detection blocks. Also the fidelity F_2 is more sensitive to proper adjustment of the HOM dip due to the unbalanced splitting ratio of $VRC_{|0\rangle}$.

Our experiment demonstrates that the fiber optics enables us to reach high interference visibilities and achieve fidelities exceeding the universal cloning limit. This setup is compatible with fiber-based communications and can be also used as an asymmetric phase-covariant cloner simply by changing the splitting ratios of VRCs (see Ref. [20]). However, some fiber components cause significant power losses. Although the probability of success of the cloning operation itself is relatively high, $P_{succ} = (33.5 \pm 0.3)\%$, the actual cloning rate is

very low, in our case about 60 per second, due to losses in the state-preparation and detection part of the setup.

VII. CONCLUSIONS

We constructed four experimental setups realizing symmetric phase-covariant cloning of single-photon qubits. The information is encoded either into polarization, or into spatial modes. The cloning operation is implemented probabilistically by interference of the signal photon with an ancilla photon. Three setups realized the cloning by using a special beam splitter with different transmittance for the two basis states $|0\rangle$ and $|1\rangle$. In contrast, the hybrid setup realized the cloning by an alternative approach employing two standard 50:50 beam splitters followed by state filtration introduced by polarization-dependent losses.

Table I summarizes our measurement results. The first setup represents purely free-space realization based on the Mach-Zehnder interferometer. This setup is very flexible; any required transmittance can be adjusted by tuning the Soleil-Babinet compensators. However, imperfections of individual components sum up so that the average cloning fidelity is below the semiclassical limit. The simplification of this cloning setup led to the second setup based on the specially designed beam splitter. The average cloning fidelity is close to the limit of the universal cloner. The asymmetry of the clones is not easily tunable. The main advantage is the high coincidence rate. We exceeded the limit of the universal cloner for cloning of polarization states with the third setup. It takes advantage of the perfect overlap of spatial modes in the fiber-based beam splitter (the fiber coupler) and it also uses simple encoding into polarization modes. The main disadvantage of this strategy is smaller theoretically attainable probability of success. The last setup is composed of fiber components exclusively. The fidelities measured with this setup also exceeded the universal cloning limit. In this case, the qubits were encoded into spatial modes. This type of encoding permits easy tunability of the asymmetry, but the setup composed of two Mach-Zehnder interferometers is rather sensitive to fluctuations and requires active stabilization.

[1] W. K. Wootters and W. H. Zurek, Nature (London) **299**, 802 (1982); D. Dieks, Phys. Lett. **92A**, 271 (1982).

[2] V. Bužek and M. Hillery, Phys. Rev. A **54**, 1844 (1996).

[3] V. Scarani, S. Iblisdir, N. Gisin, and A. Acín, Rev. Mod. Phys. **77**, 1225 (2005).

[4] N. J. Cerf and J. Fiurášek, in *Progress in Optics*, edited by E. Wolf (Elsevier, New York, 2006), Vol. 49, p. 455.

[5] A. Lamas-Linares, C. Simon, J. C. Howell, and D. Bouwmeester, Science **296**, 712 (2002).

[6] S. Fasel, N. Gisin, G. Ribordy, V. Scarani, and H. Zbinden, Phys. Rev. Lett. **89**, 107901 (2002).

[7] F. De Martini, D. Pelliccia, and F. Sciarrino, Phys. Rev. Lett. **92**, 067901 (2004).

[8] M. Ricci, F. Sciarrino, C. Sias, and F. De Martini, Phys. Rev. Lett. **92**, 047901 (2004).

[9] W. T. M. Irvine, A. L. Linares, M. J. A. de Dood, and D. Bouwmeester, Phys. Rev. Lett. **92**, 047902 (2004).

[10] I. Ali Khan and J. C. Howell, Phys. Rev. A **70**, 010303(R) (2004).

[11] N. Gisin and S. Massar, Phys. Rev. Lett. **79**, 2153 (1997).

[12] C. A. Fuchs, N. Gisin, R. B. Griffiths, C.-S. Niu, and A. Peres, Phys. Rev. A **56**, 1163 (1997).

[13] J. Soubusta, A. Černoch, J. Fiurášek, and M. Dušek, Phys.

[14] J. Du, T. Durt, P. Zou, H. Li, L. C. Kwek, C. H. Lai, C. H. Oh, and A. Ekert, Phys. Rev. Lett. **94**, 040505 (2005).

[15] F. Sciarrino and F. De Martini, Phys. Rev. A **72**, 062313 (2005).

[16] M. Ricci, F. Sciarrino, N. J. Cerf, R. Filip, J. Fiurášek, and F. De Martini, Phys. Rev. Lett. **95**, 090504 (2005).

[17] J. Fiurášek, Phys. Rev. A **67**, 052314 (2003).

[18] A. Černoch, L. Bartůšková, J. Soubusta, M. Ježek, J. Fiurášek, and M. Dušek, Phys. Rev. A **74**, 042327 (2006).

[19] Z. Zhao, A.-N. Zhang, X.-Q. Zhou, Y.-A. Chen, C.-Y. Lu, A. Karlsson, and J.-W. Pan, Phys. Rev. Lett. **95**, 030502 (2005).

[20] L. Bartůšková, M. Dušek, A. Černoch, J. Soubusta, and J. Fiurášek, e-print arXiv:quant-ph/0612119.

[21] C.-S. Niu and R. B. Griffiths, Phys. Rev. A **60**, 2764 (1999).

[22] D. Bruß, M. Cinchetti, G. M. D'Ariano, and C. Macchiavello, Phys. Rev. A **62**, 012302 (2000).

[23] A. T. Rezakhani, S. Siadatnejad, and A. H. Ghaderi, Phys. Lett. A **336**, 278 (2005).

[24] R. Derka, V. Bužek, and A. K. Ekert, Phys. Rev. Lett. **80**, 1571 (1998).

[25] C. K. Hong, Z. Y. Ou, and L. Mandel, Phys. Rev. Lett. **59**, 2044 (1987).

Rev. A **69**, 052321 (2004).